World's First Predictive and Validated Yarn-level FEA Modeling of the V0-V100 Probabilistic Penetration Response of Fully-Clamped Kevlar Fabric

GAURAV NILAKANTAN

ABSTRACT

This paper presents the world's first fully validated and predictive capability to model the V_0-V_{100} probabilistic penetration response of woven aramid fabrics using a yarn-level fabric finite element model. The V_0-V_{100} curve describes the probability of complete fabric penetration as a function of projectile impact velocity. The exemplar case considered in this paper comprises of a single-layer, fully-clamped, plain-weave Kevlar fabric impacted at the center by two types of 0.22 cal projectiles: a 11-gr spherical projectile and a 17-gr FSP or fragment-simulating projectile. Each warp and fill yarn in the fabric is individually modeled using 3D finite elements. A probabilistic computational framework is developed to map in the experimentally characterized sources of statistical variability into the fabric model and then generate a numerical V_0-V_{100} curve through a series of impact simulations at varying impact velocities. This paper also reports the experimental characterization data and its statistical analysis used for model input, viz. the Kevlar yarn tensile strengths, moduli, and inter-yarn friction, and the experimental ballistic test data used for model validation.

INTRODUCTION

Aramid (e.g. Kevlar, Twaron) woven fabrics are used in body armor systems for extremity protection and as backing for the ceramic torso plates. The penetration response of armor is probabilistic and represented by a V_0-V_{100} curve that describes the probability of complete fabric penetration (0 to 100%) as a function of projectile impact velocity (V). Sources of intrinsic and extrinsic statistical variability such as filament and yarn moduli and tensile strengths, inter-yarn friction, and projectile impact location relative to the weave contribute to the fabric probabilistic penetration response and the characteristic zone of mixed results (ZMR) that is observed during experimental testing [1]. The ZMR is the region between the lowest penetrating shot velocity (V_P) and highest non-penetrating shot velocity (V_{NP}) such that $V_P < V_{NP}$.

Gaurav Nilakantan, Teledyne Scientific & Imaging, Thousand Oaks, CA 91360, U.S.A.

Two metrics often used to assess and compare the performance of body armor systems are the back-face signature (BFS) and V_{50} velocity. The V_{50} velocity, which represents the projectile impact velocity that has a 50% probability of completely penetrating the armor target, can be estimated from a relatively few number of test shots (e.g. less than a dozen). However the V_{50} metric is not a very informative parameter. Instead, velocity performance metrics at the tail of the V_0-V_{100} curve, such as the V_1 or $V_{0.1}$ velocity, provide a better metric for armor applications, but require a large number of test shots to estimate with confidence. The precise probability level is determined based on acceptable risk.

For the past two decades, a slew of finite element studies such as those reported in literature review articles [2-5] have utilized fiber-level, yarn-level, and membrane-level models to simulate the ballistic impact response of woven aramid fabrics. The entirety of these models are deterministic and therefore incapable of generating a ZMR and a V_0-V_{100} curve. The usefulness of these models is thereby limited to qualitative deterministic trends while investigating the parametric effects of material and/or weave architecture. A decade ago, the high computational cost of yarn-level fabric models fully discretized with 3D finite elements limited the size of fabric targets modeled to a single ply of ~10 cm x 10 cm; however currently available high speed computing infrastructure enables the simulation of massive 3D yarn-level fabric finite element models (>300M degrees of freedom) that are representative of realistic-sized fabric ballistic test packs, such as 24 plies of 38 cm x 38 cm [1].

Aside from the deterministic-only capability, another notable feature of the slew of fabric finite element models and ballistic impact simulation studies in the literature is the lack of quantitatively-predictive models. These deterministic models often rely on some calibration against already-available experimental ballistic test data for the purposes of demonstrating numerical results that match experimental results. Unfortunately, some of these fabric models have overly-simplistic as well as inherently deficient assumptions and physics, and often blindly rely on published experimental data for model input and/or model validation, without recognizing that the experimental data may itself contain inaccuracies and error, or be neither fully consistent nor fully compatible with the numerical fabric model under consideration. Notable examples of such deficient fabric impact studies within the United States include Batra et al. [6], Chocron et al. [7], Duan et al. [8], Grujicic et al. [9], Phoenix et al. [10], and Wang et al. [11,12]. Obviously, such models are of little practical value however they continue to be cited in academic literature and used as a basis for new works. It is often uncommon for the same research group to comprehensively execute both the experimental testing and the finite element modeling to ensure consistency, accuracy, and compatibility. In spite of the very large research funding support provided over the years in the area of fabric ballistic impact modeling by several US government agencies such as ARO (Army Research Office), ARL (Army Research Lab), NSRDEC (Natick Soldier Research, Development, and Engineering Center), ONR (Office of Naval Research), and NIST (National Institute of Standards and Technology), there still isn't a single quantitatively-predictive capability for modeling the probabilistic V_0-V_{100} penetration response of Kevlar fabrics that has emerged from the scientific community that was supported by this funding. Several international (e.g. UK, France, Singapore) research groups, supported by their respective government funding agencies, have also been actively studying the ballistic impact of woven fabrics for over a decade and have also failed to create a quantitatively-

predictive probabilistic computational capability let alone a deterministic one. However, these groups continue to actively use their deficient fabric models to conduct and report new numerical studies. Examples include Chen et al. [13], Ha-Minh et al. [14,15], Shim et al. [16,17], and Sun et al [18]. The practical importance of such studies towards real-world fabric armor design and engineering is questionable.

Somewhat recently, Nilakantan et al. [19-22] introduced a new class of probabilistic woven fabric finite element models that mapped in experimentally-characterized sources of statistical variability into the fabric model, such as statistical yarn tensile strengths. Following a procedure similar to experimental testing, a series of impact simulations at varying projectile impact velocities was then executed to determine the numerical fabric V_0-V_{100} curve. This was the very first time a yarn-level fabric finite element model could successfully generate a ZMR and a V_0-V_{100} curve. However, Nilakantan's work was not experimentally validated at the time and therefore could not be considered quantitatively predictive. Nilakantan's probabilistic computational framework was exercised to study qualitative trends on the effects of clamping conditions, projectile size and shape, inter-yarn friction, and yarn strengths on the V_0-V_{100} response of single-ply Kevlar targets

To date, there is no predictive and validated finite element simulation capability for woven aramid fabrics modeled at the yarn-level that can accurately predict the experimental V_0-V_{100} curve. In this paper, the world's first such capability is presented, considering the exemplary case of a single-ply, fully-clamped Kevlar S706 fabric target impacted by two types of 0.22 cal projectiles: a 11-gr spherical projectile and a 17-gr FSP projectile. The experimental data and its statistical analysis that has been used for model input as well as model validation is also reported.

MATERIAL AND METHODS

Experimental Testing

Kevlar S706 greige fabric is used in this study. This plain-weave architecture fabric has an areal density of 183.43 g/m^2, an approximate thickness of 0.282 mm, and a yarn span of 0.747 mm in the warp and fill directions. The nominal denier of the warp and fill Kevlar KM2 yarns is 600. Each yarn is comprised of 400 approximately circular filaments of nominal diameter 12 micron and density 1.44 g/cm^3.

The fabric targets for ballistic testing comprise of a single layer of Kevlar fabric sandwiched between two aluminum picture frames lined with abrasive anti-slip tape. The exposed area (i.e. target size) is 101.6 mm x 101.6 mm while a peripheral strip 50.8 mm wide remains sandwiched at all four sides. The target is then clamped between two thick steel plates that are bolted together. This setup helps eliminate fabric boundary slippage during testing. Figure 1 displays the setup of the ballistic test range along with the test fixture used to clamp the fabric target. High speed video cameras on the top and side are used to record the projectile impact and residual velocities as well as track oblique or curved projectile exit trajectories. A smooth bore gas gun is used to launch the projectile. Gated velocity sensors at the tip of a barrel also provide a projectile velocity, as a check to the value obtained from the high speed video image analysis. Laser cross-hairs at the end of the barrel are used to target the intended point of impact.

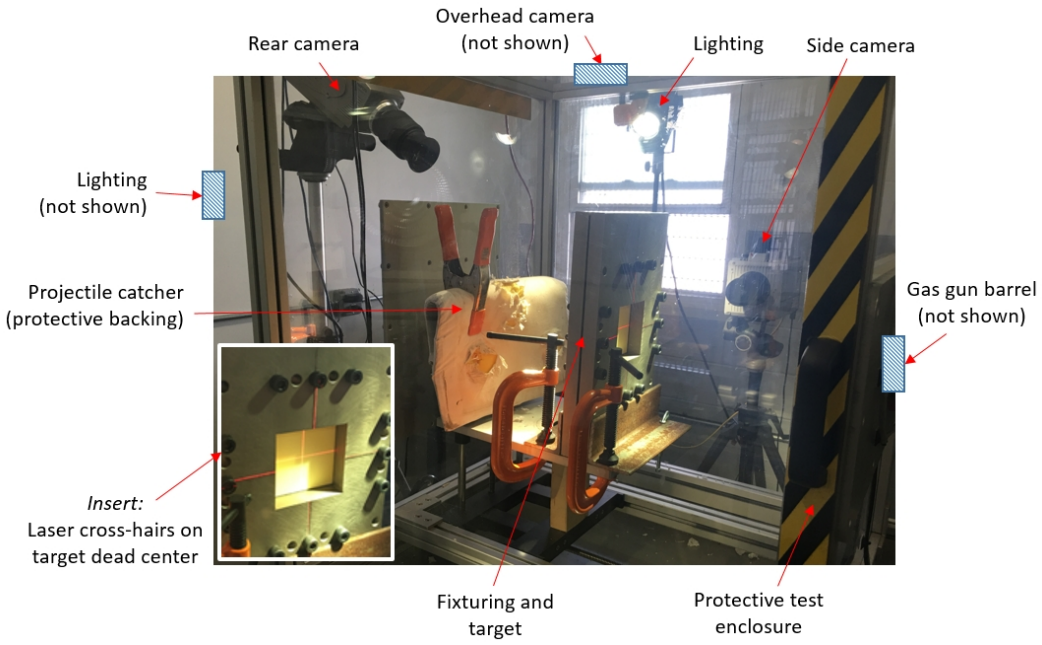

Figure 1. Ballistic test range and fabric target

The 0.22 cal, 11-gr spherical projectile has a diameter of 5.556 mm, mass of 0.691 g, and is comprised of stainless steel (grade 440C). The 0.22 cal, 17-gr FSP projectile has a diameter of 5.461 mm, length of 6.142 mm, mass of 1.096 g, and is comprised of alloy steel (grade 4340).

A total of 38 test shots are conducted for the sphere and 39 for the FSP projectile. Each fabric target is shot once at the center. The outcome (penetration = 1, non-penetration = 0) is recorded along with the projectile impact velocity (V_i), and residual velocity (V_r) in the case of penetrations. A statistical analysis is then conducted using SenTest (Neyer Software LLC [23]) to determine the V_0-V_{100} curve, represented by a Normal distribution with the mean (μ) representing the V_{50} velocity.

Figure 2 displays the 600 denier Kevlar KM2 yarn tensile moduli and strengths at a gage length of 101.6 mm, for spool-extracted and greige fabric-extracted yarns. A total of 34 spool, 55 warp, and 47 fill yarn quasi-static tensile tests were conducted. The coefficient of variation (CV) is indicative of variability and is the ratio of the standard deviation (σ) to the mean (μ) expressed as a percentage. The yarns demonstrate statistical variability in both the tensile modulus and strength. The fabric extracted yarns demonstrate weaving strength degradations with the warp yarns showing greater extents of degradation. Another source of variability considered in this study is the inter-yarn frictional interactions. These have been previously experimentally characterized by Nilakantan et al. [24] using single yarn pull-out tests at varying rates from Kevlar S706 fabric patches under varying pre-tensions. These statistical inter-yarn frictional interactions were then shown by Nilakantan et al. [25] to have significant effects on the probabilistic fabric impact performance considering partially clamped single-layer Kevlar S706 fabric targets.

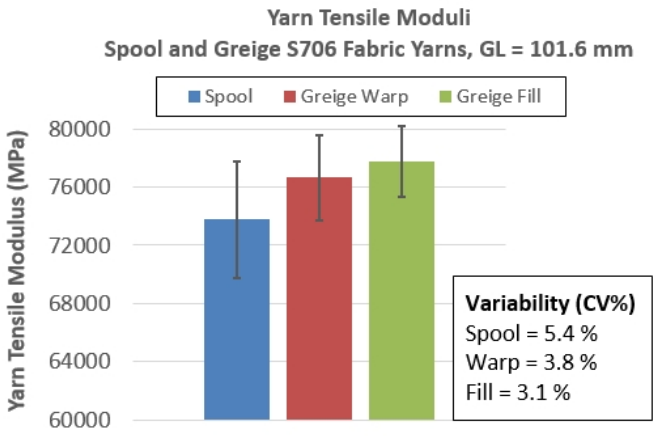

(a)

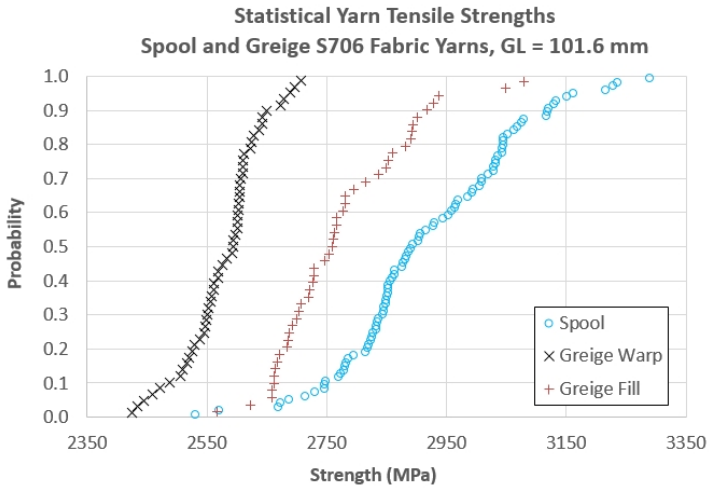

(b)

Figure 2. 600 denier Kevlar KM2 yarn properties at a gage length of 101.6 mm
(a) Yarn tensile moduli (b) Yarn tensile strengths

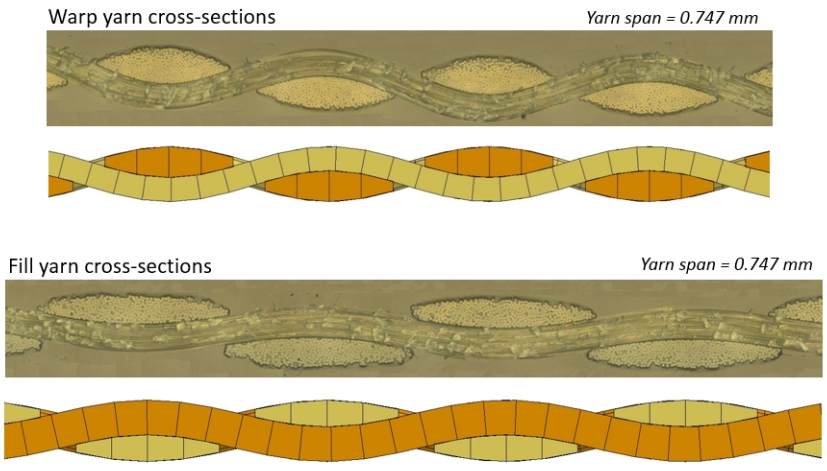

(a)

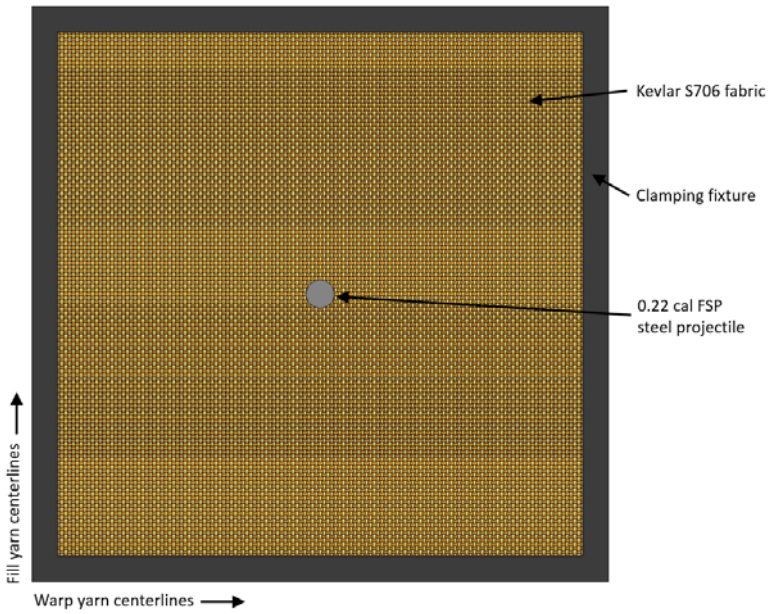

(b)

Figure 3. Fabric finite element models (a) Material and virtual yarn cross-sections
(b) Impact test setup with the 0.22 cal FSP projectile

Finite Element Modeling

Figure 3a displays optical cross-sections of the greige fabric warp and fill yarns with the corresponding FEA mesh. Detailed validation of the experimental and virtual microstructures using image analysis is available in Nilakantan et al. [26]. The yarns are discretized with single-integration point 3D hexahedral elements and assigned an orthotropic elastic material model.

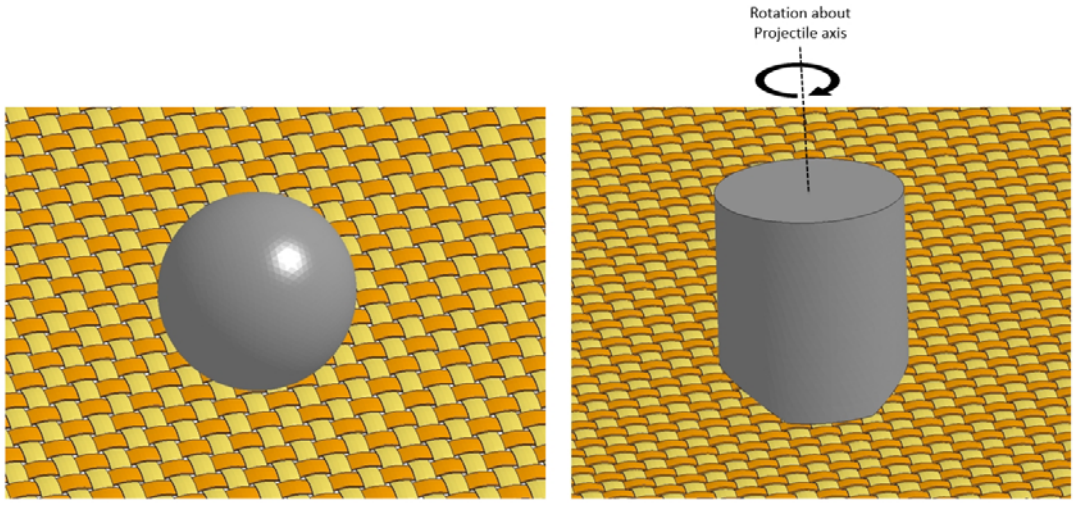

(a) (b)

Figure 4. Close-up at the impact site (a) spherical projectile (b) FSP projectile

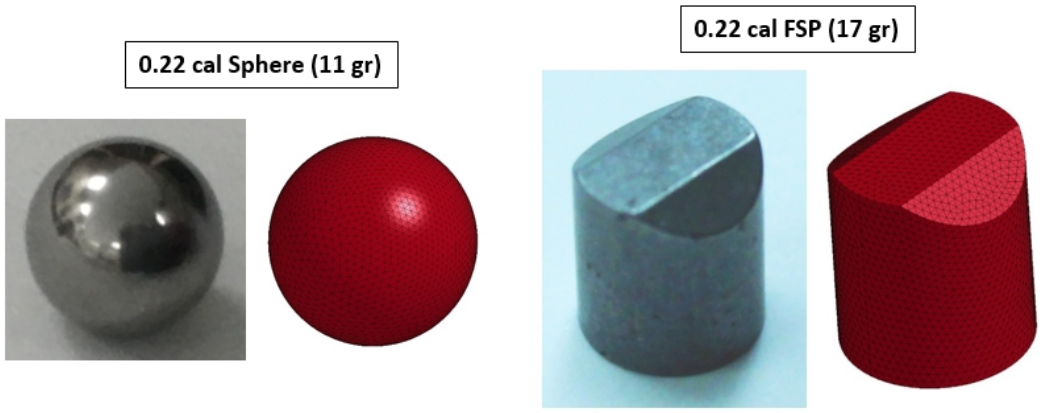

Figure 5. Experimental and virtual projectiles

Because the warp and fill yarns are represented as homogenized continua, in order to account for the filament-level architecture, the experimental material density (ρ), tensile modulus (E_{t11}), and tensile strength (σ_{t11}), (see Figure 2), must be adjusted by the respective fiber packing fractions (FPF) from the image analysis, which are respectively 69% and 89% for the warp and fill yarns. This ensures the longitudinal stress wave velocity, c (= $\sqrt{E/\rho}$), remains unchanged, and enables an accurate capturing of the fabric target mass, which is 1.9 g (experimental) and 1.8 g (virtual). Figure 3b displays the FEA setup of the impact test scenario with the FSP projectile and a 101.6 mm x 101.6 mm fabric target. While a set of clamping fixtures is modeled for visualization, the boundary nodes of the fabric model are fully constrained across all degrees of freedom to simulate a perfectly clamped boundary.

Figure 4a displays a close-up of the impact site with the spherical projectile. Figure 4b displays a corresponding close-up with the FSP projectile. The vertical axis of rotation indicates the extent of projectile yawing. The default projectile orientation is with the longer dimension of the flat impact face aligned with the fill yarn centerlines (i.e. 0° yaw) as shown in Figure 4b. A 90° and 270° rotation corresponds to alignment with the warp yarn centerlines. All impacts are normal to the fabric surface with no projectile rolling or pitching. Figure 5 compares the spherical and FSP projectiles with their corresponding FEA meshes. The projectile is discretized with tetrahedral elements and assigned to a rigid material as no projectile deformation was observed during the experimental testing.

Probabilistic Computational Framework

The sources of experimentally characterized variability need to be mapped into the FEA model in order to enable probabilistic responses. In this study, at least four sources of statistical variability have been simultaneously incorporated into the FEA model:

1. statistical yarn tensile strength
2. statistical yarn tensile modulus
3. statistical inter-yarn friction
4. random projectile impact location
5. random projectile yaw (for the FSP projectile only)

Figure 6 displays an exemplary mapping of the experimental statistical greige warp and fill yarn tensile strengths (see Figure 2b), after first being scaled by the respective FPFs, onto the individual warp and fill yarns of the fabric FEA model. In this mapping process, random numbers are used to query the statistical test data and determine the tensile strength assigned to each yarn. To verify the mapping process, a histogram of tensile warp and fill yarn strengths is generated for each fabric FEA model, scaled back to its original value by eliminating the FPF factor, and then compared to the experimental yarn strength distributions.

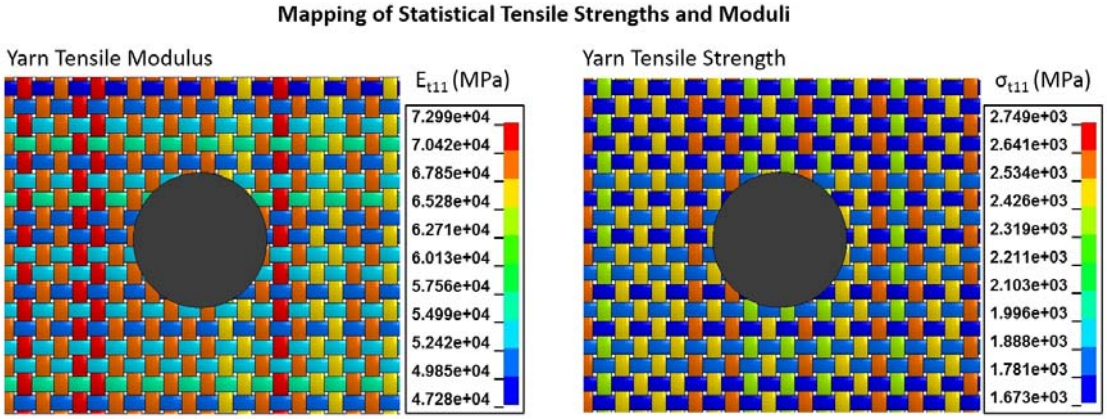

(a)

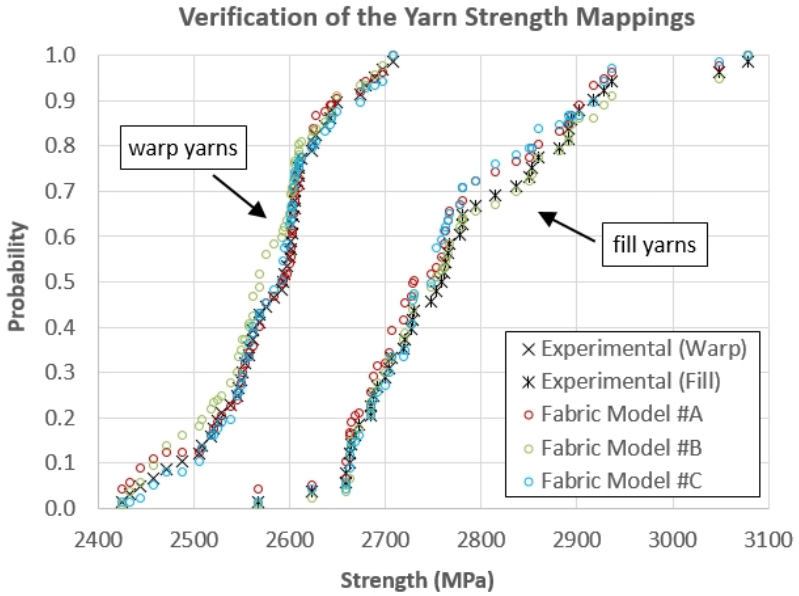

(b)

Figure 6. Mapping of statistical variability in the fabric finite element model (FSP projectile impact scenario) (a) yarn tensile modulus and strength (b) verification of the strength mappings

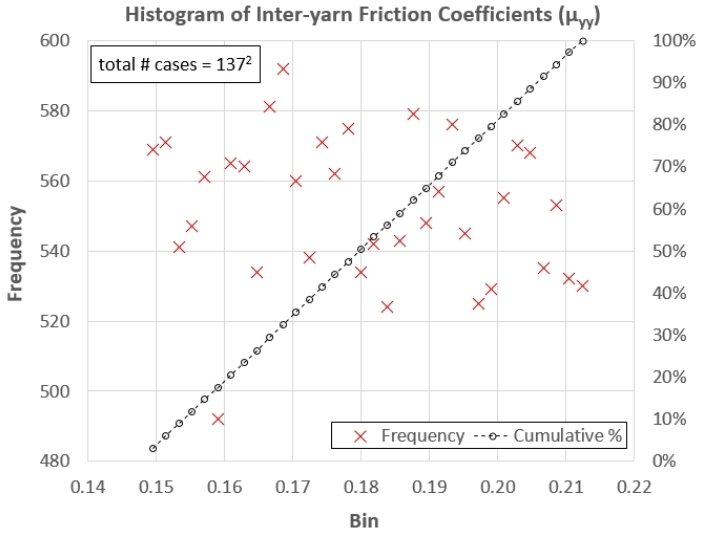

Figure 7. Mapping of statistical inter-yarn friction (FSP projectile impact scenario)

As shown in Figure 6b, the mapping process has been correctly implemented for 3 randomly selected fabric FEA models of the total 39 generated fabric FEA models for the FSP projectile impact scenario wherein each has a unique mapping. Once the strengths have been mapped, the corresponding greige warp and fill yarn tensile modulus is selected and mapped onto the yarns, since each experimental yarn tensile test provides one combination of yarn tensile strength and modulus. The process is repeated to obtain the yarn strength mappings and corresponding yarn moduli for the 38 fabric FEA models for the spherical projectile impact scenario.

Figure 7 displays the mapping of the statistical inter-yarn friction coefficients. Contact definitions are created between each of the 137 individual warp and 137 individual fill yarns in the fabric FEA model. Each warp-fill yarn contact pair, of which there are 137^2 combinations, is associated with a unique friction coefficient. The choice of inter-yarn friction coefficient is made by randomly sampling numbers within a range of 0.18 ± 0.0324. Here, 0.18 represents the baseline inter-yarn friction coefficient for Kevlar KM2. The minimum and maximum bounds selected for the range result in a standard deviation of 0.0187 and a CV of 10.4%. This CV value, which represents the variability in the statistical inter-yarn friction coefficients used for the fabric FEA model mappings, lies within the experimentally characterized CV values of 8.9% to 11.5% from the single yarn pull-out tests of greige Kevlar S706 fabrics reported in Nilakantan et al. [24]. Unlike yarn tensile strengths which typically follow a distribution such as the 3-parameter Weibull or generalized Gamma distributions resulting in the S-shaped mapping profile seen in Figure 6b, the inter-yarn friction coefficients are assumed to be randomly scattered and therefore result in a linear mapping profile (see *cumulative %* in Figure 7). In the event of warp-to-warp and fill-to-fill yarn contact, that is, two neighboring yarns of the same type contact each other which can only happen when an interlacing yarn fails, a constant friction coefficient of 0.18 is used.

Figure 8 displays the random projectile impact locations used in the 39 fabric FEA models generated for the FSP projectile impact scenario. For each random impact location, there is also a randomly assigned projectile rotation or yaw (see

Figure 4b), some of which have been shown in Figure 8 for illustration. It is impossible experimentally to precisely target the exact same spot at the fabric dead center for each test shot. Based on observations of post-tested experimental Kevlar fabric targets, a window of ±4 yarn spans (i.e. ±2.99 mm) around the dead center of the fabric FEA model was considered as the zone of possible fabric impact locations. It is also very difficult to experimentally track the precise projectile yaw just prior to impact. For each of the 39 fabric FEA models, random numbers are used to generate a set of precise projectile impact locations by sampling a range of ±2.99 mm around the fabric dead center in each direction, and to generate a set of projectile rotations by sampling a range of 0° to 360°. The precise projectile impact location relative to the fabric yarns, e.g. directly on a yarn or directly at the gap between yarns, has been previously shown by Nilakantan et al. [27,28] to have a significant effect on the deterministic impact performance of single-ply fabric targets. This effect is due to the spatial variation in local fabric weave architecture that repeats over the dimension of a unit cell. However there is also inherent variability in the fabric architecture itself, such as the yarn cross-sectional shapes, yarn centerlines trajectories, and filament packing patterns within each yarn cross-section. These sources have been presently excluded from consideration in this study. A similar set of random projectile impact locations is generated for the spherical projectile impact scenario. Because of its symmetry, projectile yaw is not a consideration for the spherical projectile. With the mapping process completed, a FEA simulation procedure very similar to the experimental procedure is adopted to generate the numerical fabric V_0-V_{100} curve for the given impact scenario. 38 fabric FEA models with unique mappings are created to compare against the 38 experimental fabric targets for the spherical projectile impact scenario (39 for the FSP projectile impact scenario). Impact simulations are then executed on each model using LS-DYNA, with varying projectile impact velocities. Each fabric model is impacted once by the projectile around its dead center. The outcome of each test (penetration = 1, non-penetration=0) along with the residual projectile velocity is used determine the next impact velocity, and finally to generate the numerical fabric V_0-V_{100} curve.

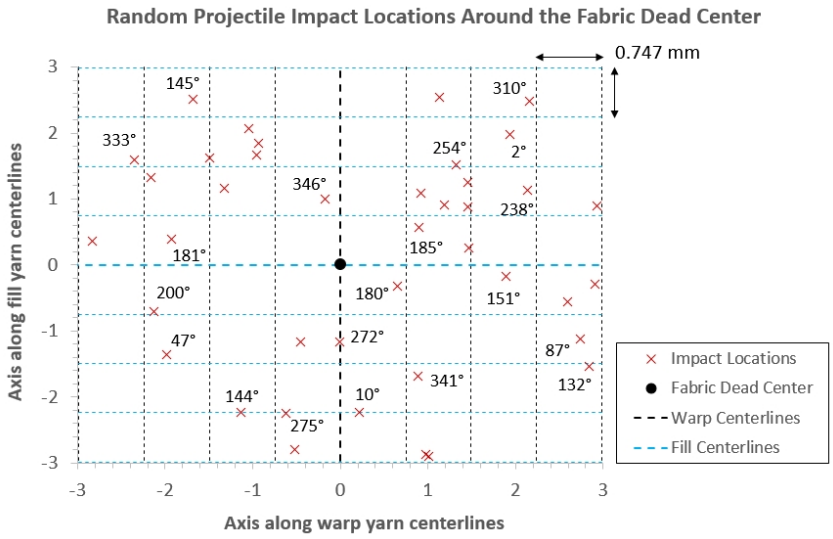

Figure 8. Random projectile impact locations and rotations (FSP projectile impact scenario)

During experimental testing with a single gas gun, test shots can only proceed one at a time. However computationally, multiple FEA simulations representing several test shots can be executed in parallel, leading to a more efficient determination of the V_0-V_{100} curve.

RESULTS AND DISCUSSION

Figure 9 compares the experimental and FEA simulation results for the 0.22 cal spherical projectile impact scenario. Figure 9a compares the experimental and numerical V_0-V_{100} curves, and there is excellent agreement between both. Figure 9a also displays the 38 experimental and numerical test shot impact velocities, with non-penetrations located at y=0.0 and penetrations at y=1.0.

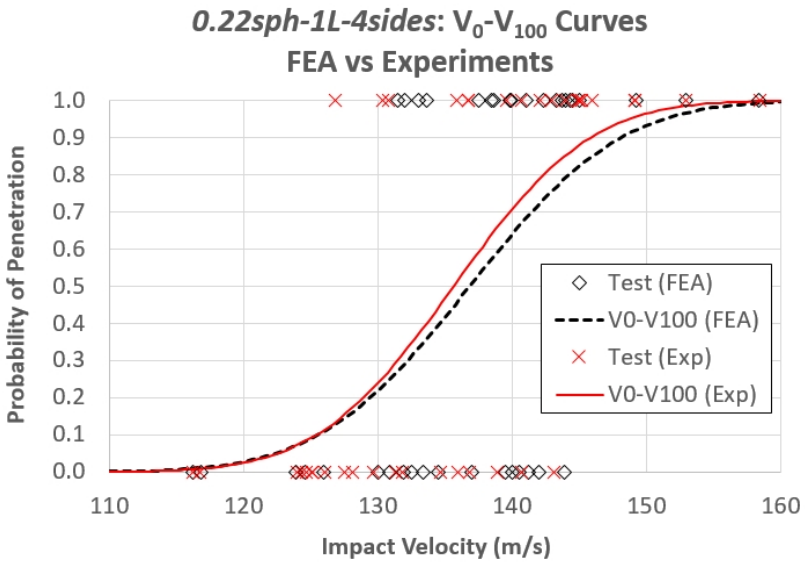

(a)

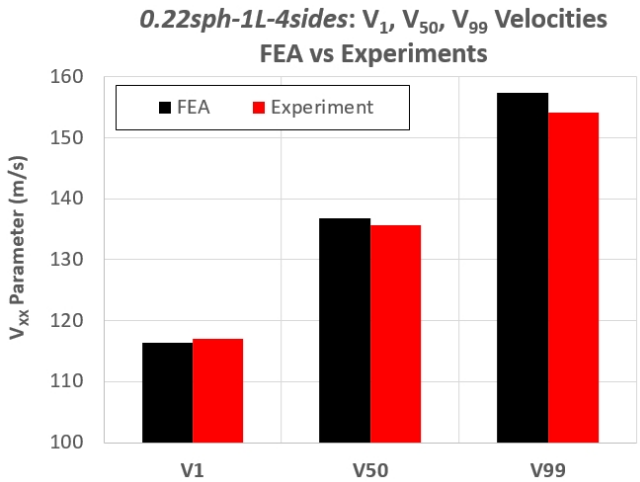

(b)

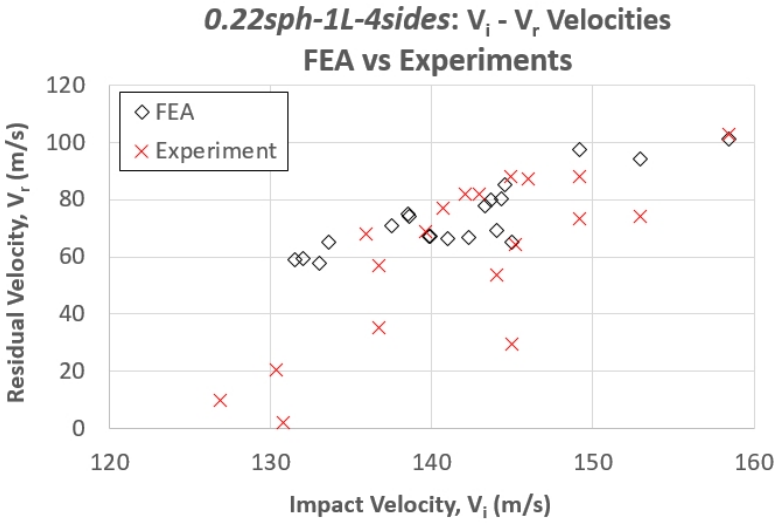

(c)

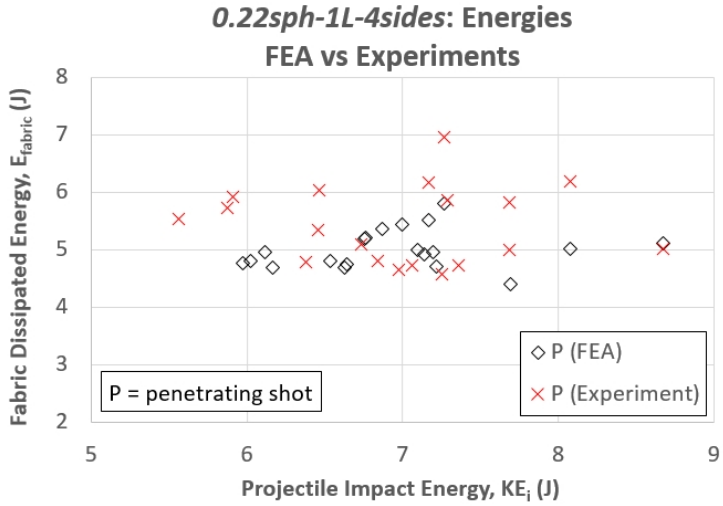

(d)

Figure 9. Comparison of experimental and FEA results for the spherical projectile impact scenario
(a) V_0-V_{100} curve and test shot data (b) V_1, V_{50}, and V_{99} velocities
(c) Vi-Vr data (d) impact and dissipated energies

There is excellent agreement between the highest non-penetrating impact velocity (experimental V_i = 143.08 m/s, numerical V_i = 143.90 m/s) and good agreement between the lowest penetrating impact velocity (experimental V_i = 126.83 m/s, numerical V_i = 131.50 m/s), while the second lowest experimental non-penetrating V_i was 130.36 m/s. Figure 9b compares the V_1, V_{50}, and V_{99} velocities, once again there is excellent agreement between the experimental and FEA simulation results. They are as follows in m/s (experimental, FEA): V_1 (117.08, 116.36), V_{50} (135.64, 136.85), and V_{99} (154.20, 157.33). Figure 9c compares the projectile residual velocities after complete fabric penetration as a function of the impact velocities, while Figure 9d displays the same set of penetrating test shots in the form of fabric dissipated energies as a function of the projectile impact kinetic energies. The fabric dissipated energy is the difference between the projectile impact and residual kinetic energies, i.e.

$\frac{1}{2}m_p(V_i^2-V_r^2)$, where m_p is the projectile mass. There is very good overall agreement between the experimental and FEA simulation V_i-V_r data as well as the fabric-projectile energy data, with the exception that the FEA simulations could not reproduce a few of the low experimental V_r values, i.e. the five test shots with a V_r < 40 m/s with one as low as 2.17 m/s.

Figure 10 similarly compares the experimental and FEA simulation results for the 0.22 cal FSP projectile impact scenario. Once again, there is excellent agreement between the experimental and numerical V_0-V_{100} curves as seen in Figure 10a. There is excellent agreement between the highest non-penetrating impact velocity (experimental V_i = 126.55 m/s, numerical V_i = 126.50 m/s) and between the lowest penetrating impact velocity (experimental V_i = 113.09 m/s, numerical V_i = 114.80 m/s), while the second lowest experimental non-penetrating V_i was 115.70 m/s. Figure 10b, which compares the compares the V_1, V_{50}, and V_{99} velocities, shows excellent agreement as follows in m/s (experimental, FEA): V_1 (106.89, 108.82), V_{50} (120.98, 121.68), and V_{99} (135.08, 134.54).

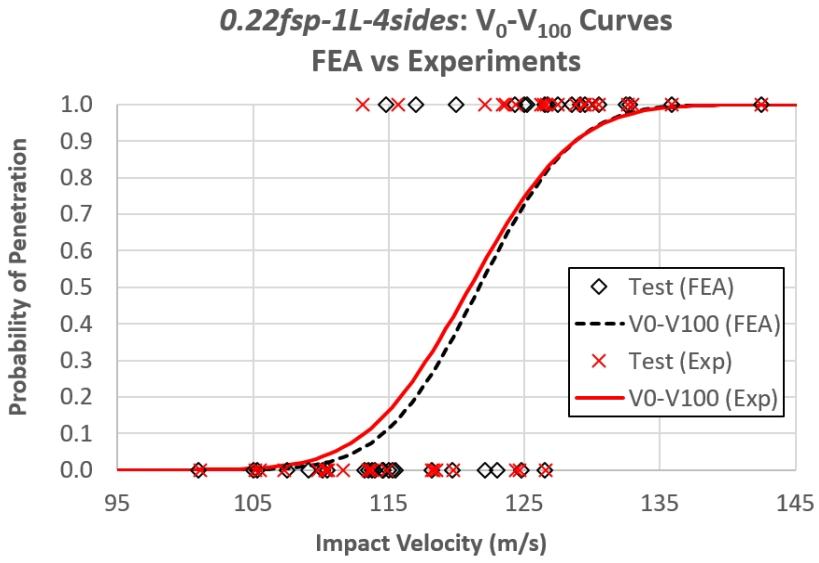

(a)

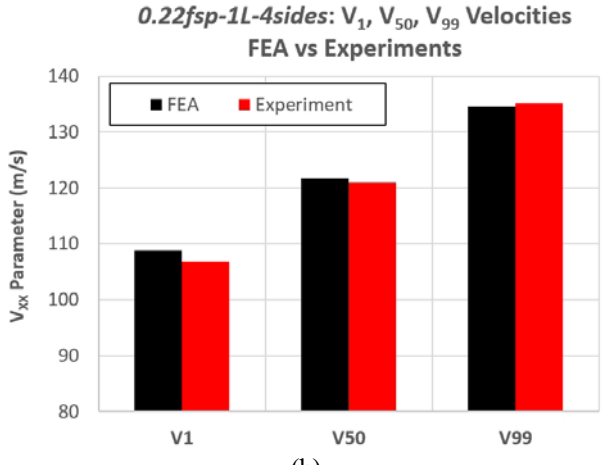

(b)

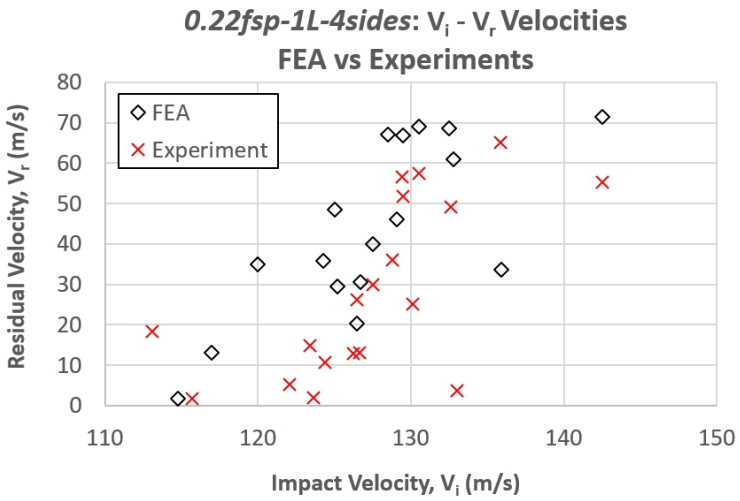

(c)

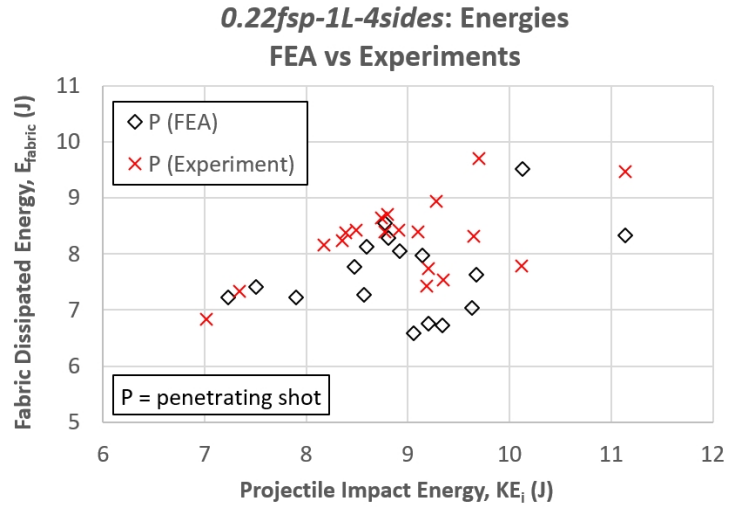

(d)

Figure 10. Comparison of experimental and FEA results for the FSP projectile impact scenario
(a) V_0-V_{100} curve and test shot data (b) V_1, V_{50}, and V_{99} velocities
(c) Vi-Vr data (d) impact and dissipated energies

Figure 10c shows excellent overall agreement between the experimental and FEA simulation V_i-V_r data as well as the fabric-projectile energy data. The observed scatter is a consequence of material and testing variability. The FEA simulations were even able to capture the lowest projectile residual velocity observed during testing (experimental V_r = 1.93 m/s, numerical V_r = 1.83), wherein the projectile barely penetrates through the fabric.

CONCLUSIONS

This work represents the world's first fully validated and predictive probabilistic penetration modeling (i.e. V_0-V_{100} response) of a woven fabric subjected to ballistic impact, utilizing a fabric finite element model with individually modeled yarns. A

probabilistic computational framework and mapping methodology was defined along with the necessary critical experimental tests at appropriate length scales and the necessary statistical analyses. Experimental validation of this probabilistic computational framework was presented for a fully-clamped, single-ply Kevlar fabric target impacted by two 0.22 cal projectiles: a sphere and a FSP. This framework can readily be extended to other Kevlar fabric weave architectures as well as other continuous-filament woven fabrics comprised of materials such as UHMWPE (Spectra, Dyneema) and aramid (Twaron). It should be noted that two key ingredients to the success of this work stem from (i) the entire set of experimental and simulation work being performed by the same researcher to ensure consistency, completeness, and a seamless flow of data and insights back and forth between models and experiments, and (ii) a sustained research effort over several years that incorporated and addressed analytical, statistical, manufacturing, experimental, and computational issues.

The development of predictive computational techniques that can explicitly account for the experimentally characterized sources of statistical variability and generate a validated probabilistic penetration response will be disruptive in the field of armor design and modeling. Such a virtual capability will enable the rapid exploration of a vast conceptual design space comprising fiber material and weave architecture, at a fraction of the cost of prototyping such designs and experimentally characterizing the ballistic impact response. The work presented here provides a strong step towards that direction. However, there will undoubtedly lie much work ahead towards extending this framework to multi-layer fabric targets wherein several other mechanisms of deformation, energy dissipation, and failure come into play, thereby necessitating further key experiments, statistical analyses, and models; this is the focus of future work.

ACKNOWLEDGEMENTS

This work was supported by Teledyne Scientific & Imaging (TS&I) Internal Research and Development (IR&D) and approved for public release under TSI-PP-17-11. GN gratefully acknowledges Dr. Bobby Brar (President, Teledyne Scientific Company) for his support of the IR&D and Mr. Robert Kinsler (HP White Laboratory Inc.) for his technical input on the high speed video analysis during ballistic testing. GN also gratefully acknowledges Dr. Eric Wetzel (US Army Research Laboratory) and Dr. James Zheng (PEO Soldier PM-SPIE) for their many helpful technical discussions, collaborations, and support over the years that contributed to the overall success of this work. The views and opinions expressed herein are those of the author and do not necessarily represent the views of TS&I or the US Government.

REFERENCES

[1] Nilakantan G, Nutt S. State of the art in the deterministic and probabilistic ballistic impact modeling of soft body armor: filaments to fabrics. American Society for Composites 29th Technical Conference, San Diego, CA, USA September 8-10, 2014.

[2] Cheeseman BA, Bogetti TA. Ballistic impact into fabric and compliant composite laminates. Composite Structures 2003;61:161-173.

[3] Tabiei A, Nilakantan G. Ballistic impact of dry woven fabric composites: A review. Applied Mechanics Reviews 2008;61(1):010801-010813.
[4] David NV, Gao XL, Zheng JQ. Ballistic resistant body armor: Contemporary and prospective materials and related protection mechanisms. Applied Mechanics Reviews 2009;62:1-20.
[5] Sockalingam S, Chowdhury SC, Gillespie JW, Keefe M. Recent advances in modeling and experiments of Kevlar ballistic fibrils, fibers, yarns and flexible woven textile fabrics – a review. Text.Res.J. 2016 05/02; 2017/04:0040517516646039.
[6] Zhang GM, Batra RC, Zheng J. Effect of frame size, frame type, and clamping pressure on the ballistic performance of soft body armor. Composites: Part B 2008;39:476-489.
[7] Chocron S, Figueroa E, King N, Kirchdoerfer T, Nicholls AE, Sagebiel E, et al. Modeling and validation of full fabric targets under ballistic impact. Composites Sci.Technol. 2010 11/15;70(13):2012-22.
[8] Duan Y, Keefe M, Bogetti TA, Powers B. Finite element modeling of transverse impact on a ballistic fabric. International Journal of Mechanical Sciences 2006;48:33-43.
[9] Grujicic M, Hariharan A, Pandurangan B, Yen CF, Cheeseman BA, Wang Y, et al. Fiber-level modeling of dynamic strength of Kevlar KM2 ballistic fabric. Journal of Materials Engineering and Performance 2011;DOI 10.1007/s11665-011-0006-1.
[10] Eken S, Phoenix SL, Yavuz AK. Computational model for woven fabrics subjected to ballistic impact by a spherical projectile. American Society for Composites 31st Technical Conference, Williamsburg, VA, USA September 19-22, 2016.
[11] Wang Y, Miao Y, Swenson D, Cheeseman BA, Yen C, LaMattina B. Digital element approach for simulating impact and penetration of textiles. Int.J.Impact Eng. 2010 5;37(5):552-60.
[12] Wang Y, Miao Y, Huang L, Swenson D, Yen C, Yu J, et al. Effect of the inter-fiber friction on fiber damage propagation and ballistic limit of 2-D woven fabrics under a fully confined boundary condition. Int.J.Impact Eng. 2016 11;97:66-78.
[13] Wang Y, Chen X, Young R, Kinloch I. Finite element analysis of effect of inter-yarn friction on ballistic impact response of woven fabrics. Composite Structures 2016;135:8-16.
[14] Ha-Minh C, Imad A, Boussu F, Kanit T, Crepin D. Numerical study on the effects of yarn mechanical transverse properties on the ballistic impact behaviour of textile fabric. The Journal of Strain Analysis for Engineering Design 2012;47(7):524-534.
[15] Ha-Minh C, Boussu F, Imad A, Kanit T, Crepin D. Multi-scale model to predict the ballistic impact behavior of multi-layer plain-woven fabrics. Int.J.Comput.Methods 2014 06/01; 2017/07;11(03):1343011.
[16] Zeng XS, Tan VBC, Shim VPW. Modelling inter-yarn friction in woven fabric armour. International Journal for Numerical Methods in Engineering 2006;66(8):1309-1330.
[17] Tapie E, Guo YB, Shim VPW. Yarn mobility in woven fabrics – a computational and experimental study. International Journal of Solids and Structures 2016;80:212-26.
[18] Sun D, Chen X, Lewis E, Wells G. Finite element simulation of projectile perforation through a ballistic fabric. Textile Research Journal 2012;83(14):1489-1499.
[19] Nilakantan G, Keefe M, Wetzel ED, Bogetti TA, Gillespie Jr. JW. Computational modeling of the probabilistic impact response of flexible fabrics. Composite Structures 2011;93:3163-3174.
[20] Nilakantan G, Keefe M, Wetzel ED, Bogetti TA, Gillespie Jr. JW. Effect of statistical yarn tensile strength on the probabilistic impact response of woven fabrics. Composites Science and Technology 2012;72(2):320-329.
[21] Nilakantan G, Wetzel ED, Bogetti TA, Gillespie Jr. JW. Finite element analysis of projectile size and shape effects on the probabilistic penetration response of high strength fabrics. Composite Structures 2012;94(5):1846-1854.
[22] Nilakantan G, Gillespie Jr. JW. Ballistic impact modeling of woven fabrics considering yarn strength, friction, projectile impact location, and fabric boundary condition effects. Composite Structures 2012;94(12):3624-3634.
[23] Neyer BT. A D-optimality-based sensitivity test. Technometrics 1994;36(1):61-70.
[24] Nilakantan G, Gillespie Jr. JW. Yarn pull-out behavior of plain woven Kevlar fabrics: Effect of yarn sizing, pull-out rate, and fabric pre-tension. Composite Structures 2013;101:215-224.
[25] Nilakantan G, Merrill R, Keefe M, Gillespie Jr. JW, Wetzel ED. Experimental investigation of the role of frictional yarn pull-out and windowing on the probabilistic impact response of Kevlar fabrics. Composites Part B: Engineering 2015;68:215-229.

[26] Nilakantan G, Cox B, Sudre O. Generation of realistic stochastic virtual microstructures using a novel thermal growth method for woven fabrics and textile composites. American Society for Composites 32nd Technical Conference, West Lafayette, IN, USA October 22-25, 2017.
[27] Nilakantan G, Nutt S. Effects of clamping design on the ballistic impact response of soft body armor. Composite Structures 2014;108:137-150.
[28] Nilakantan G, Nutt S. Effects of fabric target shape and size on the V50 ballistic impact response of soft body armor. Composite Structures 2014;116:661-669.